A Model for Single-Substrate Trimolecular Enzymatic Kinetics

Wei Chen[†] and Cheng Zhu[†‡*]
[†]Woodruff School of Mechanical Engineering and [‡]Coulter Department of Biomedical Engineering, Georgia Institute of Technology, Atlanta, Georgia

ABSTRACT We developed a kinetic model for a single-substrate trimolecular enzymatic system, where a receptor binds and stretches a substrate to expose its cleavage site, allowing an enzyme to bind and cleave it into product. We demonstrated that the general kinetics of the trimolecular enzymatic system is more complex than the Michaelis-Menten kinetics. Under a limiting condition when the enzyme-substrate binding is in fast equilibrium, the enzymatic kinetics of the trimolecular system reduces to the Michaelis-Menten kinetics. In another limiting case when the receptor dissociates negligibly slowly from the substrate, the trimolecular system is simplified to a bimolecular system, which follows the Michaelis-Menten equation if and only if there is no enzyme-substrate complex initially. We applied this model to a particular trimolecular system important to hemostasis and thrombosis, consisting of von Willebrand factor (substrate), platelet glycoprotein Ibα (receptor), and ADAMTS13 (enzyme). Using parameters from independent experiments, our model successfully predicted published data from two single-molecule experiments and fitted/predicted published data from an ensemble experiment.

INTRODUCTION

Enzymatics is a central topic of biology and biophysics because of its universal involvement in biological processes. Traditionally, population assays are used to study ensemble-averaged enzymatic kinetics, many of which can be described by the Michaelis-Menten kinetics (1). The development of new techniques such as atomic force microscopy (AFM) and optical tweezers has enabled researchers to study enzymatic kinetics at the single-molecule level. For example, English et al. (2) studied the kinetics of individual β-galactosidase by a single-molecule fluorescent assay and showed that the Michaelis-Menten equation still holds for a single enzyme that stochastically turns substrates into products one at a time. Wiita et al. (3) applied AFM to study disulfide bond reduction by thioredoxin and found that force changed the reduction rate. Combining AFM with molecular dynamics simulations, Puchner et al. (4) found strong evidence suggesting that titin kinase may act as a biological force sensor. Recently, Zhang et al. (5) and Wu et al. (6) investigated the force-induced unfolding and cleavage of the A2 domain of von Willebrand factor (VWF) by the enzyme A Disintegrin And Metalloprotease with a ThromboSpondin type 1 motifs 13 (ADAMTS13) using optical tweezers and AFM, respectively, and demonstrated that the VWF A2 domain may also serve as a biological force sensor.

Rapidly increasing data from single-molecule experiments call for the development of appropriate models for the analysis and understanding of the underlying mechanisms of the kinetic processes. Kou et al. (7) developed a model for a single-enzyme system in which an enzyme repeatedly turns substrates into products one molecule at a time. It was found that the reciprocal average turnover time of the single-enzyme reaction still follows the Michaelis-Menten equation. However, this work did not analyze the opposite situation, i.e., a single substrate being catalyzed by surrounding enzyme molecules into product, which is the case in the single-molecule experiments of the VWF cleavage by ADAMTS13 (5,6). Zhang et al. (5) adapted the single-molecule Michaelis-Menten equation developed by Kou et al. (7) by replacing the concentration of the substrate with that of the enzyme. We will show that this is valid only under certain conditions that were not met in the experiments of Zhang et al. (5). Furthermore, the model of Kou et al. (7) accounts only for a bimolecular enzyme-substrate system. Many enzymatic systems are more complex, consisting of three or more players such as the case of VWF cleavage by ADAMTS13 under physiological conditions. To address these limitations, we developed a model for a trimolecular mechanoenzymatic system in which a receptor binds a substrate and stretches it to facilitate its proteolysis by an enzyme. Although the mathematical formulation is completely general, the model will be exemplified using a specific system, consisting of the platelet glycoprotein (GP) Ibα, its ligand VWF, and the VWF-cleaving enzyme ADAMTS13.

The GPIbα-VWF-ADAMTS13 system is crucial to physiological hemostasis and pathological thrombosis. Upon stimulation, endothelial cells secret prothrombogenic ultralarge VWF (ULVWF) that often attaches to the vascular surface (8). Circulating platelets bind ULVWF via GPIbα to the VWF A1 domain (9), which applies force to and may induce unfolding of the VWF A2 domain to expose the cryptic proteolytic site at the Tyr^{1605}-Met^{1606} peptide bond (10), thereby allowing ADAMTS13 to cleave the ULVWF multimers into smaller-sized plasma VWF multimers (11). Either

Submitted November 28, 2009, and accepted for publication January 8, 2010.

*Correspondence: cheng.zhu@bme.gatech.edu

Wei Chen's present address is Department of Bioengineering, University of Washington, Seattle, WA 98195-5013.

Editor: Patrick Loria.

0006-3495/10/05/1957/9 $2.00

doi: 10.1016/j.bpj.2010.01.020

dysfunction of ADAMTS13 or mutations in the A2 domain cause severe diseases such as thrombotic thrombocytopenia purpura (12) or type 2A von Willebrand disease (VWD) (13).

Using the model, we demonstrated that, for an enzyme-substrate biomolecular system, the reciprocal average turnover time of the single-substrate reaction still follows the Michaelis-Menten equation if and only if there is no enzyme-substrate complex initially. The initial conditions are critical for correctly predicting the measured kinetics. In general, the kinetics of a trimolecular system is much more complex than the Michaelis-Menten kinetics. We applied our model to two single-molecule experiments (5,6), and successfully predicted the data based on kinetic rates measured from independent experiments (14–16). In addition, our model was able to predict an ensemble platelet-VWF agglutination experiment (17).

RESULTS

Model and analysis

Model development and general solution

Our model for the binding and enzymatic kinetics of a trimolecular system is illustrated in Fig. 1. The main model includes a GPIbα receptor molecule on the platelet surface, a monomeric unit of a (UL)VWF substrate molecule anchored on the vascular surface, and an ADAMTS13 enzyme molecule in the plasma. The platelet bound to VWF is pushed by the flowing blood, which pulls on the tethered VWF to unfold the A2 domain with a rate k_u. ADAMTS13 binds VWF with on- and off-rates k_{+1} and k_{-1}, respectively. Platelet detachment from the vascular surface can occur via GPIbα dissociation from VWF A1 (with an off-rate k_r) or ADAMTS13 cleavage of VWF A2 (with a cleavage rate k_c). Here a single rate k_r has been assumed for GPIbα to dissociate from VWF or VWF-ADAMTS13 because Wu et al. (6) have demonstrated that the force-dependent off-rates of GPIbα-VWF bonds are identical with or without VWF binding to ADAMTS13. After detachment, the platelet enters the blood stream; therefore, it cannot rebind the same VWF.

Let us first focus on the events after VWF has already associated with GPIbα and been unfolded. The events of GPIbα-VWF binding and VWF unfolding, as depicted in the dashed box in Fig. 1, will be studied later with an application to experiment. Before platelet detachment, a VWF molecule exists in one of two states:

1. Bound with both GPIbα and ADAMTS13 (*blue* VWF in Fig. 1, with a probability p_1); or
2. Bound with GPIbα only (*red* VWF in Fig. 1, with a probability p_2).

Binding of ADAMTS13 to and dissociation from VWF result in reversible conversion between the two states. Platelet detachment via either GPIbα dissociation from VWF (with or without ADAMTS13 bound to it) or ADAMTS13 cleavage of VWF yields a third state (*green* VWF in Fig. 1, with a probability $p_0 = 1 - p_1 - p_2$), resulting in irreversible net loss of the probability p_1 and p_2. The master equations for the kinetics of the first two states are

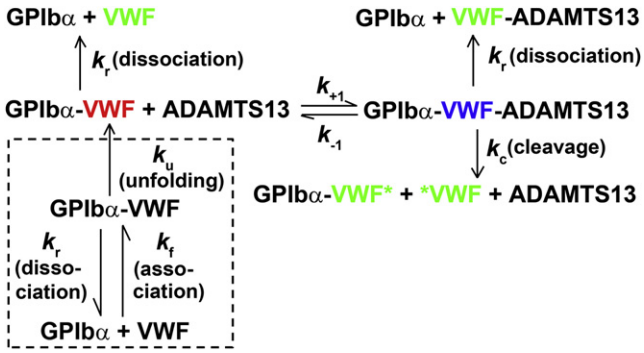

FIGURE 1 Model for binding and enzymatic kinetics of the GPIbα-VWF-ADAMTS13 trimolecular system. The k_f, k_r, k_u, k_c, k_{+1}, and k_{-1} are kinetic rates (see text for details). VWF* and *VWF present the cleaved VWF products. Three states of VWF are highlighted in different colors. Dashed box includes the kinetic processes of GPIbα-VWF binding and VWF unfolding, which is added to the main model only for treating the experiment of agglutination of platelet-VWF.

$$\begin{cases} \dfrac{dp_1}{dt} = -(k_{-1} + k_r + k_c)p_1 + k_{+1}c\,p_2 \\ \dfrac{dp_2}{dt} = k_{-1}p_1 - (k_{+1}c + k_r)p_2 \end{cases}, \tag{1}$$

where t is time and c is free ADAMTS13 concentration.

Take $t = 0$ as the moment when the A2 domain is just unfolded so that ADAMTS13 can access the otherwise cryptic proteolytic site in A2. Assume that VWF-ADAMTS13 binding is in equilibrium because ADAMTS13 can bind VWF A3 and/or A2 in the native, folded structure (18,19). Consequently, when GPIbα binds VWF, it binds either to a standalone VWF or to a VWF-ADAMTS13 complex. After a standalone VWF binds GPIbα, it still needs to bind ADAMTS13 for it to be cleaved. Thus, the initial conditions for Eq. 1 that satisfy the normalization requirement $p_1 + p_2 = 1$ are

$$\begin{aligned} p_1 &= \frac{c}{c + K_D}, \\ p_2 &= \frac{K_D}{c + K_D}, \end{aligned} \qquad t = 0 \tag{2}$$

where $K_D = k_{-1}/k_{+1}$ is the equilibrium dissociation constant of VWF-ADAMTS13 binding.

The solution of Eqs. 1 and 2 can be expressed as

$$\begin{cases} p_1 = A\,\exp[-(k_r + \lambda_1)t] + B\,\exp[-(k_r + \lambda_2)t] \\ p_2 = C\,\exp[-(k_r + \lambda_1)t] + D\,\exp[-(k_r + \lambda_2)t] \end{cases}, \tag{3}$$

where

$$A = C\,(c/K_D - \lambda_1/k_{-1}), \tag{4a}$$

$$B = D\ (c/K_D - \lambda_2/k_{-1}), \tag{4b}$$

$$C = \frac{\lambda_2}{(1 + c/K_D)(\lambda_2 - \lambda_1)}, \tag{4c}$$

$$D = \frac{\lambda_1}{(1 + c/K_D)(\lambda_1 - \lambda_2)}, \tag{4d}$$

and

$$\lambda_{1,2} = \frac{k_{-1}}{2}\left[\left(1 + \frac{c}{K_D} + \frac{k_c}{k_{-1}}\right) \mp \sqrt{\left(1 + \frac{c}{K_D} + \frac{k_c}{k_{-1}}\right)^2 - 4\frac{c}{K_D}\frac{k_c}{k_{-1}}}\right]. \tag{5}$$

The cumulative probability for a platelet to detach before time t is $p_0 = 1 - p_1 - p_2$. The probability density for detachment to occur at t can be calculated as

$$\begin{aligned} f(t) &= dp_0/dt \\ &= (A + C)(k_r + \lambda_1)\exp[-(k_r + \lambda_1)t] + (B + D) \\ &\quad \times (k_r + \lambda_2)\exp[-(k_r + \lambda_2)t]. \end{aligned} \tag{6}$$

Parametric analysis

To characterize the mathematical properties of the model, we plot $f(t)$ versus t in Fig. 2, which illustrates the effects of kinetic rates and enzyme concentration on $f(t)$.

First, increasing k_{-1} shifts $f(t)$ toward a broader distribution with more tethered platelets with longer lifetimes (Fig. 2 *A*). This is because the increase of k_{-1} tilts the equilibrium of the VWF-ADAMTS13 binding toward a state in which fewer VWF molecules are bound with ADAMTS13. With less A2 cleavage by ADAMTS13, more platelets remain attached for longer times. Second, increasing k_c shifts $f(t)$ toward a narrower distribution with more tethered platelets having short lifetimes (Fig. 2 *B*). This resulted from faster ADAMTS13 cleavage of VWF A2. Third, increasing k_r has a similar effect because faster dissociation of GPIbα from VWF A1 shortens the lifetimes of the tethered platelets (Fig. 2 *C*). Fourth and finally, increase in ADAMTS13 concentration tilts the equilibrium of VWF-ADAMTS13 binding toward a state in which more VWF molecules are bound with ADAMTS13 to facilitate cleavage and, therefore, $f(t)$ is shifted leftward with more tethered platelets having shorter lifetimes (Fig. 2 *D*). Evidently, $f(t)$ is much more sensitive to k_c and k_r, which vary in much smaller ranges but induce larger changes in $f(t)$.

Special cases

Because of the stochastic nature of single-bond dissociation kinetics and single-molecule enzymatics, experimental data are random, which are often analyzed by taking average of the lifetimes of the tethered platelet, $\langle t\rangle$. This is the first moment of $f(t)$ and can be calculated as

$$\begin{aligned} \langle t\rangle &= \int_0^\infty t f(t)dt \\ &= \frac{(1 + c/K_D)[1 + (K_M + c)k_{+1}/k_r] - c\,k_c/(K_D k_r)}{k_r(1 + c/K_D)\left[1 + c\,k_c k_{+1}/k_r^2 + (K_M + c)k_{+1}/k_r\right]}, \end{aligned} \tag{7}$$

where $K_M = (k_{-1} + k_c)/k_{+1}$ is the Michaelis constant.

Several special cases are of particular interest. Setting $c = 0$ reduces Eq. 7 to $\langle t\rangle_0 = 1/k_r$. This is expected because the trimolecular system is reduced to that of bimolecular dissociation of GPIbα from VWF A1 (17).

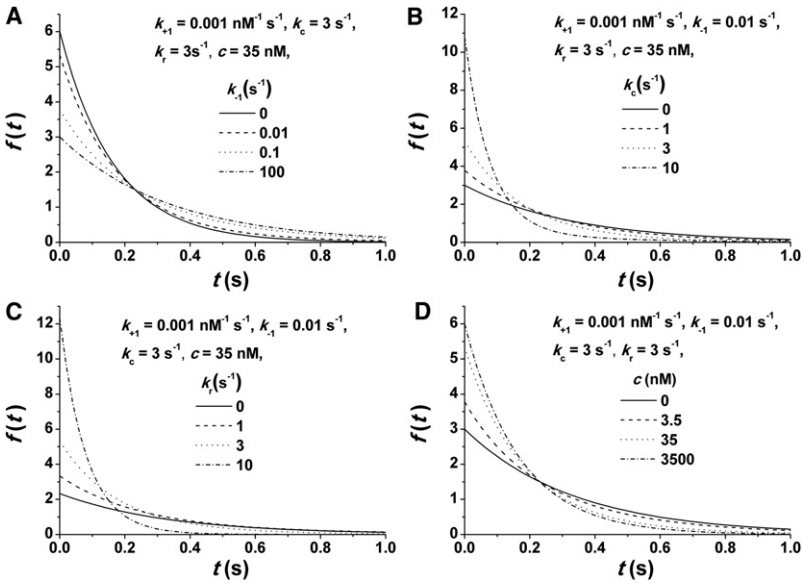

FIGURE 2 Probability density of the lifetimes of the tethered platelets, $f(t)$, plotted versus k_{-1}, the dissociation rate of the ADAMTS13-VWF interaction (*A*), k_c, the cleavage rate of VWF by ADAMTS13 (*B*), k_r, the dissociation rate of the GPIbα-VWF interaction (*C*), and c, the ADAMTS13 concentration (*D*).

If $k_{-1} \sim k_{+1}c \rightarrow 0$, i.e., VWF-ADAMTS13 binding proceeds with very slow kinetics, then Eq. 7 becomes

$$1/\langle t\rangle - 1/\langle t\rangle_0 = ck_ck_r/[(c + K_D)k_r + k_cK_D]. \quad (8)$$

If $k_{-1} \sim k_{+1}c \rightarrow \infty$, i.e., VWF-ADAMTS13 binding proceeds with very fast kinetics and reaches equilibrium in much shorter time than the enzymatic kinetics, then Eq. 7 becomes

$$1/\langle t\rangle - 1/\langle t\rangle_0 = ck_c/(c + K_M). \quad (9)$$

This is of the same form as the Michaelis-Menten equation except that the substrate concentration is replaced by the enzyme concentration. This result is expected because this limiting case makes the same quasi-steady-state assumption as does the Michaelis-Menten kinetics.

If $k_r \rightarrow 0$, i.e., GPIbα does not dissociate from VWF, the trimolecular system is reduced to a bimolecular system of enzymatic cleavage. Equation 7 then becomes

$$1/\langle t\rangle = ck_c(c + K_D)/\left(c^2 + 2K_Dc + K_MK_D\right). \quad (10)$$

This is different from the Michaelis-Menten equation (Eq. 9 with $1/\langle t\rangle_0 = k_r = 0$), which was obtained by Kou et al. (7), even if we replace the enzyme concentration with the substrate concentration. The apparent discrepancy is due to the different initial conditions used by Kou et al., which assume no enzyme-substrate complex initially, i.e.,

$$\begin{aligned} p_1 &= 0, \\ p_2 &= 1. \end{aligned} \quad t = 0 \quad (11)$$

The solution of Eqs. 1 and 11 can be expressed as

$$\begin{cases} p_1 = \dfrac{k_{+1}c}{(\lambda_2 - \lambda_1)}\{\exp[-(k_r + \lambda_1)t] - \exp[-(k_r + \lambda_2)t]\} \\ p_2 = \dfrac{1}{(\lambda_2 - \lambda_1)}\{(k_{-1} + k_c - \lambda_1)\exp[-(k_r + \lambda_1)t] \\ \qquad - (k_{-1} + k_c - \lambda_2)\exp[-(k_r + \lambda_2)t]\} \end{cases} . \quad (12)$$

The average lifetime of the tethered platelets is

$$\langle t\rangle = \int_0^\infty t\mathrm{d}p_0 = \frac{c + K_M + k_r/k_{+1}}{c\,k_c + (c + K_M + k_r/k_{+1})k_r}. \quad (13)$$

If $k_r \rightarrow 0$, Eq. 13 becomes

$$1/\langle t\rangle = ck_c/(c + K_M), \quad (14)$$

which is identical to the Michaelis-Menten equation. Together with the result of Kou et al. (7), Eq. 14 shows that, if there is no enzyme-substrate complex at $t = 0$, the kinetics of a bimolecular enzyme-substrate system always follows the Michaelis-Menten equation regardless of whether the single molecule of interest is the enzyme or the substrate.

Randomness parameter

Stochasticity due to fluctuations is a feature of single-molecule enzymatics that is absent in ensemble enzymatics. The complete information of the stochastic process is embedded in the probability density function $f(t)$ from which simple descriptive statistics such as average lifetime $\langle t\rangle$ can be obtained. In addition to the first moment, the second moment of $f(t)$ can be calculated as

$$\begin{aligned} \langle t^2\rangle &= \int_0^\infty t^2 f(t)\mathrm{d}t \\ &= 2(A + C)/(k_r + \lambda_1)^2 + 2(B + D)/(k_r + \lambda_2)^2. \end{aligned} \quad (15)$$

Using Eqs. 7 and 15, the standard deviation $\sigma(t)$ of lifetime t can be calculated according to

$$\sigma(t) = \sqrt{\langle t^2\rangle - \langle t\rangle^2}. \quad (16)$$

Furthermore, a randomness parameter r (7,20) is defined as

$$r = \left(\langle t^2\rangle - \langle t^2\rangle\right)/\langle t\rangle^2. \quad (17)$$

To illustrate its characteristics, r is plotted versus ADAMTS13 concentration c in Fig. 3 with $k_{+1} = 0.001\ \mathrm{nM}^{-1}\ \mathrm{s}^{-1}$, $k_{-1} = 0.01\ \mathrm{s}^{-1}$, $k_c = 3\ \mathrm{s}^{-1}$, and $k_r = 3\ \mathrm{s}^{-1}$. At $c = 0$, there is no ADAMTS13 to bind and cleave VWF; the platelet detachment becomes a one-step Poisson process, so $r = 1$ (7). As $c \rightarrow \infty$, VWF tends to become always bound with ADAMTS13. The detachment is also a one-step Poisson process, although it includes two pathways: GPIbα dissociation and ADAMTS13 cleavage. Therefore, r also converges to unity. However, at the intermediate concentrations, $r > 1$ because of the interconversion of the two states of VWF

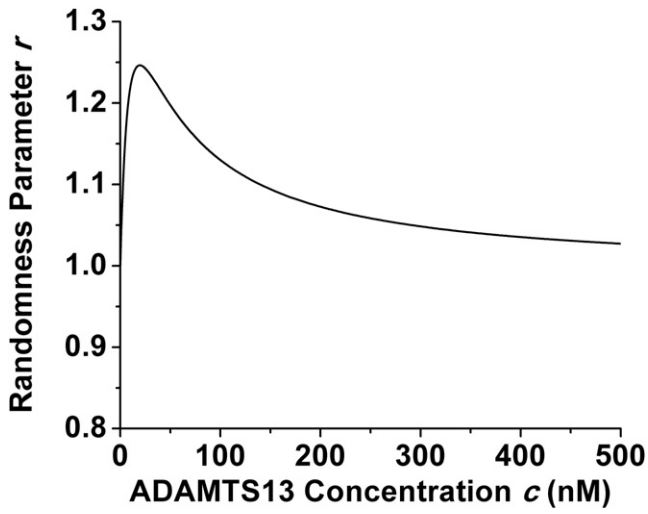

FIGURE 3 Randomness parameter r versus ADAMTS13 concentration c with $k_{+1} = 0.001\ \mathrm{nM}^{-1}\ \mathrm{s}^{-1}$, $k_{-1} = 0.01\ \mathrm{s}^{-1}$, $k_c = 3\ \mathrm{s}^{-1}$, and $k_r = 3\ \mathrm{s}^{-1}$.

(with and without binding to ADAMTS13) before platelet detachment.

Comparison with experiments

Predicting the kinetics of a VWF A2-ADAMTS13 bimolecular system

Using our model, we first analyzed the kinetics of the VWF A2-ADAMTS13 bimolecular system studied by Zhang et al. (5). In their experiment, GPIbα was eliminated by using a recombinant A2 domain engineered with molecular handles to strongly attach its C- and N-termini to the optical tweezers ($k_r \to 0$), which reduces the trimolecular system to a bimolecular system. Single A2 domains were stretched to unfold with optical tweezers to allow ADAMTS13 to cleave the Tyr^{1605}-Met^{1606} peptide bond (10). Using the kinetic rates measured independently by Zanardelli et al. (16), where $K_M = 1.61\ \mu M$, $k_c = 0.14\ s^{-1}$, and $K_D = 20$ nM, the predictions of Eqs. 10 and 14 for the reciprocal average time required for cleavage are plotted in Fig. 4 versus ADAMTS13 concentration along with the data from Zhang et al. (5). The data are well predicted by Eq. 10 but not by Eq. 14, suggesting that Eq. 2 is a more appropriate initial condition than Eq. 11. In fact, the experiment was performed in the continuous presence of ADAMTS13, allowing equilibrium binding with folded A2 before stretching and cleavage (19).

In addition to substituting independently measured kinetic rates into a model to predict experiment, one can also fit a model to data to evaluate kinetic rates. Zhang et al. (5) fitted their data by Eq. 14, which has two parameters (K_M and k_c). Their best-fit K_M is an order-of-magnitude smaller than the independently measured value (16). This discrepancy may be explained by the use of an inappropriate initial condition that no ADAMTS13 was bound to A2 before unfolding. By comparison, our model (Eq. 10) includes three parameters (K_D, K_M, and k_c). Because the data from Zhang et al. (5) are limited (only three points), we fixed one parameter (K_M) to obtain a more robust estimate of the other two (K_D and k_c). If more data becomes available, our model will be able to evaluate all three parameters.

As shown in Table 1, K_D (but not k_c) strongly depends on the chosen value of K_M. This is expected because k_c determines the saturated reaction rate when $c \to \infty$ whereas K_M and K_D determine how quickly the reaction rate changes versus ADAMTS13 concentration. The goodness-of-fit is assessed by two parameters: adjusted R^2 (the closer to 1 the better) and standard error of mean (SE) of the fitted parameters (normally smaller than mean for a good fit). Although fixing $K_M = 160$ nM (the value reported by Zhang et al. (5) based on fitting their data with Eq. 14) to conditionally fit the data with Eq. 10 yielded a high adjusted R^2, the best-fit K_D (526 nM) is an order-of-magnitude greater than the measured value (16) and the SE is too large (597 nM). By comparison, two fits with $K_M = 1000$ and 1610 nM are better than others because they yielded adjusted $R^2 > 0.9$ and also small SE compared to the mean for the best-fit parameters. Because of the limited data, we were unable to determine a unique fit to distinguish the K_M and K_D values in the last two rows of Table 1, but both are comparable to the measurements of Zanardelli et al. (16), indicating that Eq. 10 is consistent with experiments. This analysis also suggests that the K_M and K_D values reported by Zanardelli et al. (16) can better describe the data of Zhang et al. (5).

Predicting the kinetics of a GPIbα-VWF A1A2A3-ADAMTS13 trimolecular system

Next, we applied our model to predict the kinetics of the GPIbα-VWF A1A2A3-ADAMTS13 trimolecular system studied by Wu et al. (6). The authors used AFM to stretch and unfold A1A2A3-tridomains, which were then cleaved by ADAMTS13. Using the kinetic rates from Ai et al. (14) and Raife et al. (15) ($K_M = 5.81\ \mu M$, $k_c = 4.43\ s^{-1}$, and $K_D = 4.6$ nM) and GPIbα-VWF dissociation rate measured without ADAMTS13 treatment (6) ($k_r = 3.06\ s^{-1}$), we calculated the average lifetime $\langle t \rangle$ by Eq. 7 and the standard deviation $\sigma(t)$ by Eq. 16. It is evident from Fig. 5 that our predictions are in a good agreement with the measurements of Wu et al. (6). Here, we used a set of kinetic rates that are different from those used to predict the experiment of

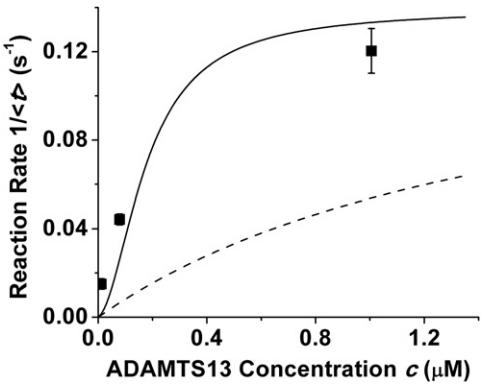

FIGURE 4 Comparison between the predicted and measured enzymatic kinetics of a VWF-ADAMTS13 bimolecular system. Predictions were calculated from Eqs. 10 (*solid curve*) and 14 (*dashed curve*) with measured kinetic rates ($K_M = 1.61\ \mu M$, $k_c = 0.14\ s^{-1}$, and $K_D = 20$ nM) from Zanardelli et al. (16). Experimental data (*points*, mean ± SE) are from Zhang et al. (5).

TABLE 1 Summary of best-fit parameters

K_M (nM)	Best-fit k_c (s^{-1}) (mean ± SE)	Best-fit K_D (nM) (mean ± SE)	Adjusted R^2
1	0.10 ± 0.11	118 ± 1330	0.17
10	0.08 ± 0.04	−264 ± 210	0.89
100	0.14 ± 0.12	269 ± 1540	0.97
160	0.17 ± 0.03	526 ± 597	0.99
1000	0.12 ± 0.01	11.5 ± 6.35	0.95
1610	0.12 ± 0.01	6.88 ± 3.73	0.94

Equation 10 was fit to the data in Fig. 4 with indicated K_M.

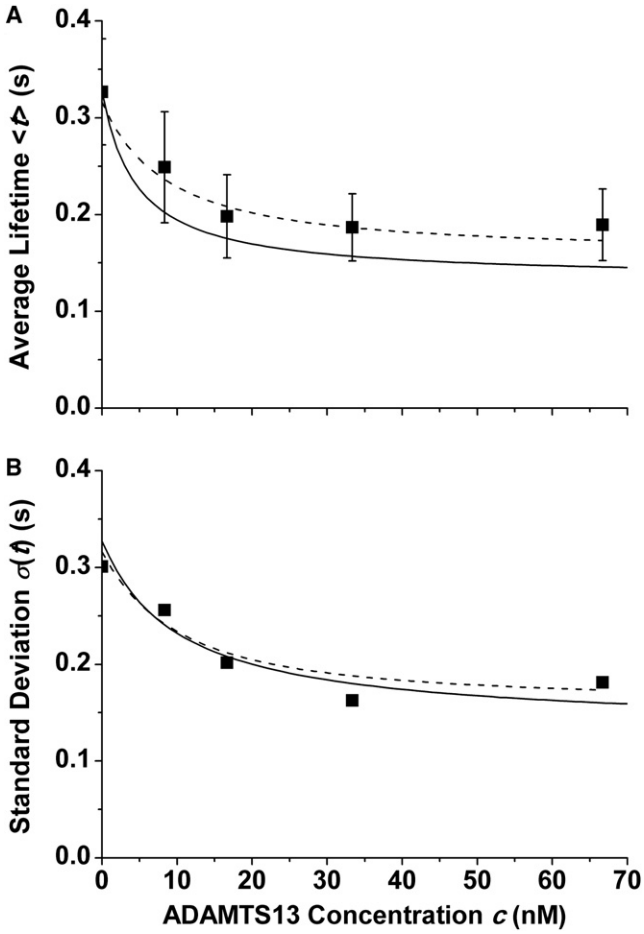

FIGURE 5 Comparison between the calculated and measured enzymatic kinetics of a GPIbα-VWF-ADAMTS13 trimolecular system. Predictions (*solid curves*) and fitting (*dashed curves*) of the averages (*A*) and the standard deviations (*B*) of lifetimes were calculated by Eqs. 7 and 16. For predictions, the kinetic rates ($K_M = 5.81$ μM, $k_c = 4.43$ s^{-1}, $K_D = 4.6$ nM) are from the literature (14,15) and the GPIbα-VWF dissociation rate ($k_r = 3.06$ s^{-1}) is from Wu et al. (6). Experimental data (*points*, mean ± SE) are also from Wu et al. (6).

Zhang et al. (5) because different VWF constructs were used in the two studies (A1A2A3 tridomain versus isolated A2 domain). Wu et al. (6) fitted the average lifetime $\langle t \rangle$ with Eq. 8 that does not contain K_M, which is approximate in the limiting case of slow VWF-ADAMTS13 binding. In an attempt to obtain the missing information, we used the general solution—both Eqs. 7 and 16—to fit the average lifetime $\langle t \rangle$ and the standard deviation $\sigma(t)$ simultaneously, yielding $K_M = 24.1 \pm 25.7$ nM, $k_c = 3.31 \pm 0.73$ s^{-1}, $K_D = 11.6 \pm 12.6$ nM, and $k_r = 3.16 \pm 0.13$ s^{-1}. The best-fit k_c, K_D, and k_r are similar to the published values measured by independent experiments (6,14,15). However, the best-fit K_M is two-orders-of-magnitude smaller than the measurement (15,16,21). This discrepant K_M may be explained by the lack of sensitivity of our fitting to K_M. Indeed, simultaneously fitting the average lifetime $\langle t \rangle$ and the standard deviation $\sigma(t)$ in Fig. 5 by Eqs. 7 and 16 with K_M fixed in a wide range from 1 nM to 10 μM returns similar k_c, K_D, and k_r values and similar goodness-of-fit (Table 2). This analysis explains why the published K_M value (5.81 μM) was able to predict the data (Fig. 5). It also explains why Eq. 8 was able to fit the data despite the fact that it does not contain K_M (6). In fact, reliable K_M value cannot be obtained by fitting Eqs. 7 and 16 to the data in Fig. 5 because the experiment was done under the condition in which Eq. 8 is valid.

Fitting/predicting an ensemble experiment of platelet-VWF agglutination

As another experimental validation, we applied the model to the experiment of Yago et al. (17) in which beads coated with type 2B VWD mutant A1A2A3-tridomain fragments of VWF were mixed with platelets in a flow chamber to allow agglutination between beads and platelets via GPIbα-VWF binding. Addition of ADAMTS13 reduced the extent of agglutination because the platelet-bead aggregates could be broken-up by cleavage of A2 in addition to GPIbα-VWF A1 dissociation. We assume:

1. that the aggregates were comprised of mostly platelet-bead doublets;
2. that each doublet was linked by a single GPIbα-VWF A1 bond; and
3. that unfolded A2 did not refold.

Agglutination occurred in a shear flow, requiring the addition of GPIbα-VWF A1 binding and A2 unfolding to our kinetics model (Fig. 1, *dash box*). Following Long et al. (22), the doublet formation frequency f_p, or the number of doublets formed in a unit time per particle, is

$$f_p = \frac{4\pi}{3} N_p (R_b + R_p)^3 A_c m_r m_l k_f, \qquad (18)$$

where N_p is the concentration of platelets, R_b and R_p are the respective radii of the bead and platelet (assumed as a sphere of 1 μm radius), A_c is the contact area, m_r and m_l are the respective densities of receptors and ligands, and k_f is forward rate of GPIbα-VWF association. Assuming that dissociation of the GPIbα-VWF bond and unfolding of the A2 domain both follow first-order kinetics, the probabilities for a doublet formed at τ_1 not to break up at t and for its A2 domain not to unfold at t are $\exp[-k_r(t - \tau_1)]$ and

TABLE 2 Summary of best-fit parameters

K_M (nM)	Best-fit k_r (s^{-1}) (mean ± SE)	Best-fit k_c (s^{-1}) (mean ± SE)	Best-fit K_D (nM) (mean ± SE)	Adjusted R^2
1	3.16 ± 0.18	2.26 ± 0.39	6.06 ± 1.40	0.80
10	3.15 ± 0.13	2.85 ± 0.67	13.2 ± 14.7	0.88
100	3.18 ± 0.13	2.99 ± 0.58	6.59 ± 3.25	0.89
1000	3.18 ± 0.15	2.87 ± 0.64	5.20 ± 2.66	0.86
5810	3.19 ± 0.15	2.86 ± 0.65	5.06 ± 2.62	0.86
10,000	3.19 ± 0.15	2.85 ± 0.65	5.05 ± 2.62	0.86

Equations 7 and 16 were fit to the data in Fig. 5 with indicated K_M.

$\exp[-k_u(t - \tau_1)]$, respectively. The fraction of doublets formed during the period (t_1, t) that remain unbroken and with a native A2 domain at time t is

$$p_{s1} = \int_{t_1}^{t} f_p \exp[-(k_r + k_u)(t - \tau_1)]d\tau_1 = \frac{f_p}{(k_r + k_u)}\{1 - \exp[-(k_r + k_u)(t - t_1)]\}. \quad (19)$$

The probabilities for a doublet formed at τ_1 not to break up at τ_2 and for its A2 domain to unfold in the interval $(\tau_2, \tau_2 + d\tau_2)$ are $\exp[-k_r(\tau_2 - \tau_1)]$ and $k_u \exp[-k_u(\tau_2 - \tau_1)]d\tau_2$, respectively. The probability for a doublet with an unfolded A2 domain at τ_2 to remain unbroken at t is $p_1(t - \tau_2) + p_2(t - \tau_2)$, as given by Eq. 3. Therefore, the fraction of doublets formed during the period (t_1, t) that remain unbroken and with an unfolded A2 domain at time t is

$$\begin{aligned} p_{s2} &= \int_{t_1}^{t}\int_{\tau_1}^{t} f_p k_u \exp[-(k_r + k_u)(\tau_2 - \tau_1)][p_1(t - \tau_2) \\ &\quad + p_2(t - \tau_2)]d\tau_2 d\tau_1 \\ &= f_p \{1/(k_r + k_u)[k_u(A + C)/(k_r + \lambda_1) \\ &\quad + k_u(B + D)/(k_r + \lambda_2)] + 1/(k_r + k_u) \\ &\quad \times [k_u(A + C)/(k_u - \lambda_1) + k_u(B + D) \\ &\quad /(k_u - \lambda_2)]e^{-(k_r + k_u)(t_2 - t_1)} - k_u(A + C) \\ &\quad /[(k_u - \lambda_1)(k_r + \lambda_1)]e^{-(k_r + \lambda_1)(t_2 - t_1)} - k_u(B + D) \\ &\quad /[(k_u - \lambda_2)(k_r + \lambda_2)]e^{-(k_r + \lambda_2)(t_2 - t_1)}\}. \end{aligned} \quad (20)$$

The total fraction of surviving doublets p_s at time t is the sum of Eqs. 19 and 20,

$$p_s = p_{s1} + p_{s2}. \quad (21)$$

Let $t_1 = 5\pi/(6G)$ be the average encounter duration between a bead and a platelet, $t_2 = 6L/(hG)$ be the average time for the particles to transit through the flow chamber of length L and height h at a wall shear rate G, and t_3 be the lumped time for the particles to enter and exit the flow chamber. Substituting t_1 and $t = t_2 + t_3$ into Eq. 21 then allows us to calculate the fraction of surviving doublets at the exit of the flow chamber, as measured in the agglutination experiment of Yago et al. (17).

We first analyzed the data measured in the absence of ADAMTS13 from Yago et al. (17). Under the condition $c = 0$, Eq. 21 is simplified to

$$p_s = (f_p/k_r)[1 - \exp(-k_r(t_2 - t_1))]. \quad (22)$$

Equation 22 was fit to the data without ADAMTS13 using an unfolding rate of $k_u = 0.0007 \exp(F/1.1)\ s^{-1}$ (5) and a dissociation rate of $k_r = 1.448 \exp(F/29.412)\ s^{-1}$ with tether force $F = 0.0047 R_b R_p G$ pN (17). The fitting yielded good agreement with the experiment (Fig. 6). Two parameters resulted from the fitting: $A_c m_r m_l k_f = 24.2\ s^{-1}$ and $t_3 = 0.505$ s. These two parameters were used along with the measured kinetic rates from Ai et al. (14) and Raife et al. (15) to calculate the fraction of surviving doublets p_s with ADAMTS13 according to Eq. 21. The calculation agreed well with the data measured in the presence of ADAMTS13 from Yago et al. (17) (Fig. 6). Thus, the same kinetic rates measured from independent experiments of Ai et al. (14) and Raife et al. (15) were able to predict the mechanoenzymatics of the GPIbα-VWF A1A2A3-ADAMTS13 trimolecular system in both single-molecule (Fig. 5) and ensemble (Fig. 6) experiments.

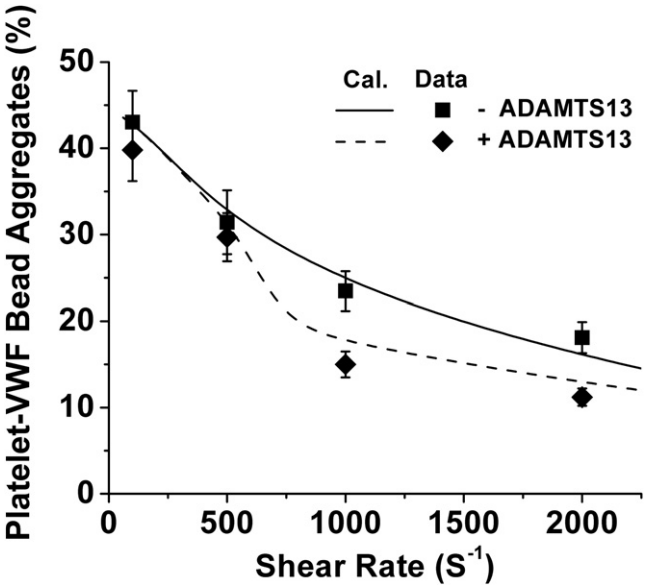

FIGURE 6 Comparison of platelet agglutination between calculations (*curves*) and experiments (*points*). Calculations are based on Eqs. 21 and 22. The kinetic rates ($K_M = 5.81\ \mu M$, $k_c = 4.43\ s^{-1}$, $K_D = 4.6$ nM) are from the literature (14,15). Experimental data and parameters ($L = 20$ mm, $h = 0.25$ mm, $c = 33.35$ nM, $N_p = 10^8\ mL^{-1}$, $R_b = 3\ \mu m$, and $R_p = 1\ \mu m$) are from Yago et al. (17).

DISCUSSION

We described a kinetic model for a single-substrate trimolecular enzymatic system and used it to analyze the interplay of GPIbα, VWF, and ADAMTS13 in both single-molecule and ensemble experiments, yielding good agreement. In general, the kinetics of the trimolecular system is more complex than the Michaelis-Menten kinetics. In the limiting case in which dissociation of GPIbα from VWF is negligible, the trimolecular system is simplified to a bimolecular system. We demonstrated that the biomolecular system follows the Michaelis-Menten equation if and only if there is no enzyme-substrate complex initially, as in the model of Kou et al. (7). However, this is not true in the case of ADAMTS13

cleavage of VWF because previous studies show that ADAMTS13 can bind the VWF A2 domain before A2 is unfolded (19). In addition, ADAMTS13 binds the VWF A3 domain (18). It is therefore reasonable to assume that the binding between ADAMTS13 and VWF is in equilibrium during incubation before VWF is stretched and unfolded. ADAMTS13 is a multidomain protein and its VWF binding and catalytic sites are located at different domains (23), so it is assumed that the initial ADAMTS13-VWF complex is cleavage competent. Indeed, with the equilibrium assumption, our model gives a much better prediction than the Michaelis-Menten equation, as shown in Fig. 4. Nevertheless, with the absence of any enzyme-substrate complex as the initial condition, the kinetics of both single substrate and single enzyme systems converges to the Michaelis-Menten equation, which demonstrates the symmetry of substrate and enzyme in a bimolecular enzyme-substrate system.

For the more general GPIbα-VWF-ADAMTS13 trimolecular system where the Michaelis-Menten equation is not applicable, our model also gives reasonable predictions to the data of Wu et al. (6) (Fig. 5). Interestingly, here we used a set of kinetic rates from Ai et al. (14) and Raife et al. (15) whereas another set from Zanardelli et al. (16) was used to predict the data of Zhang et al. (5). The biggest difference between the two sets of kinetic rates is the cleavage rate k_c. The value from the former set is one order-of-magnitude larger than that from the latter set. However, the difference in the parameter is due to the difference in experimental data. One possible reason for the discrepant results could be the different VWF constructs used in the two studies. In the study of Zhang et al. (5), only A2 is included in the VWF construct. However, an A1A2A3-tridomain construct was used by Wu et al. (6). A1 and/or A3 may regulate the ADAMTS13 cleavage of A2 by increasing k_c. Another possible reason could be the different levels of stretching force. The stretching force is ~5 pN in the study of Zhang et al. (5). By comparison, the stretching force spans from 10 to 80 pN in the study of Wu et al. (6). At lower force, unfolded A2 could be more coiled and more difficult for ADAMTS13 to access, explaining a smaller k_c. Furthermore, the two sets of kinetic rates used for calculations were measured with different VWF constructs. The set from Ai et al. (14) and Raife et al. (15) was measured using VWF73 whereas the set from Zanardelli et al. (16) was measured using VWF115. VWF115 includes additional N-terminal residues of A2, which could protect the cleavage site from access of ADAMTS13 and thus reduces the cleavage rate k_c.

Wu et al. (6) fitted the average lifetime using Eq. 8, which is an approximate equation for the slow VWF-ADAMTS13 binding condition. They could not get K_M because of its absence in Eq. 8. In an attempt to obtain all four independent kinetic parameters, K_M, k_c, K_D, and k_r, we used the general solution as described by Eqs. 7 and 16 to fit the average value and the standard deviation of lifetimes from Wu et al. (6) simultaneously. We obtained comparable k_c, K_D, and k_r to previous fitting (6) and experimental (6,14,15) results. However, the best-fit K_M was two orders-of-magnitude smaller than the measured value (15,16,21). Because the standard error of K_M is larger than its mean, the fitting is not good from a mathematical standpoint. Moreover, the fitting is not sensitive to K_M. When K_M was fixed in a wide range, the fitting yielded similar results for other kinetic rates (Table 2). Therefore, we concluded that the data of Wu et al. (6) are not sufficient to obtain K_M because the experiments were performed under the condition in which the results are indifferent to K_M.

Combined with the work of Long et al. (22), our model also successfully predicted the ensemble experiment of the platelet-VWF agglutination (17). Considering the complexity of the experiment, the good agreement of our simple model with the data is quite impressive. More importantly, using our model to fit experimental data, the agglutination assay provides a new method to estimate the kinetic rates of the ADAMTS13 cleavage of VWF.

In conclusion, our kinetic model of a trimolecular enzymatic system has extended the scope of the simpler bimolecular model of Kou et al. (7). In principle, our model can analyze experimental data for any trimolecular enzymatic system to quantitatively estimate kinetic rates and to reveal underlying mechanisms.

We thank Jiangguo Lin, Tao Wu, and Tadayuki Yago for providing experimental data of their published work (6,17).

This work was supported by National Institutes of Health grants No. HL091020 and No. HL093723.

REFERENCES

1. Michaelis, L., and M. L. Menten. 1913. The kinetics of the inversion effect. *Biochem. Z.* 49:333–369.
2. English, B. P., W. Min, …, X. S. Xie. 2006. Ever-fluctuating single enzyme molecules: Michaelis-Menten equation revisited. *Nat. Chem. Biol.* 2:87–94.
3. Wiita, A. P., R. Perez-Jimenez, …, J. M. Fernandez. 2007. Probing the chemistry of thioredoxin catalysis with force. *Nature*. 450:124–127.
4. Puchner, E. M., A. Alexandrovich, …, M. Gautel. 2008. Mechanoenzymatics of titin kinase. *Proc. Natl. Acad. Sci. USA*. 105:13385–13390.
5. Zhang, X. H., K. Halvorsen, …, T. A. Springer. 2009. Mechanoenzymatic cleavage of the ultralarge vascular protein von Willebrand factor. *Science*. 324:1330–1334.
6. Wu, T., J. Lin, …, C. Zhu. 2010. Force-induced cleavage of single VWFA1A2A3 tridomains by ADAMTS-13. *Blood*. 115:370–378. 10.1182/blood-2009–1103–210369.
7. Kou, S. C., B. J. Cherayil, …, X. S. Xie. 2005. Single-molecule Michaelis-Menten equations. *J. Phys. Chem. B*. 109:19068–19081.
8. Dong, J. F., J. L. Moake, …, J. A. López. 2002. ADAMTS-13 rapidly cleaves newly secreted ultralarge von Willebrand factor multimers on the endothelial surface under flowing conditions. *Blood*. 100:4033–4039.
9. Huizinga, E. G., S. Tsuji, …, P. Gros. 2002. Structures of glycoprotein Ibα and its complex with von Willebrand factor A1 domain. *Science*. 297:1176–1179.
10. Dent, J. A., S. D. Berkowitz, …, Z. M. Ruggeri. 1990. Identification of a cleavage site directing the immunochemical detection of molecular

abnormalities in type IIA von Willebrand factor. *Proc. Natl. Acad. Sci. USA*. 87:6306–6310.

11. Auton, M., M. A. Cruz, and J. Moake. 2007. Conformational stability and domain unfolding of the Von Willebrand factor A domains. *J. Mol. Biol.* 366:986–1000.
12. Levy, G. G., W. C. Nichols, …, H. M. Tsai. 2001. Mutations in a member of the ADAMTS gene family cause thrombotic thrombocytopenic purpura. *Nature*. 413:488–494.
13. Michiels, J. J., A. Gadisseur, …, H. van Vliet. 2005. Characterization, classification, and treatment of von Willebrand diseases: a critical appraisal of the literature and personal experiences. *Semin. Thromb. Hemost.* 31:577–601.
14. Ai, J., P. Smith, …, X. L. Zheng. 2005. The proximal carboxyl-terminal domains of ADAMTS13 determine substrate specificity and are all required for cleavage of von Willebrand factor. *J. Biol. Chem.* 280: 29428–29434.
15. Raife, T. J., W. Cao, …, X. L. Zheng. 2009. Leukocyte proteases cleave von Willebrand factor at or near the ADAMTS13 cleavage site. *Blood.* 114:1666–1674.
16. Zanardelli, S., J. T. Crawley, …, D. A. Lane. 2006. ADAMTS13 substrate recognition of von Willebrand factor A2 domain. *J. Biol. Chem.* 281:1555–1563.
17. Yago, T., J. Lou, …, C. Zhu. 2008. Platelet glycoprotein Ibα forms catch bonds with human WT vWF but not with type 2B von Willebrand disease vWF. *J. Clin. Invest.* 118:3195–3207.
18. Dong, J. F., J. L. Moake, …, M. A. Cruz. 2003. ADAMTS-13 metalloprotease interacts with the endothelial cell-derived ultra-large von Willebrand factor. *J. Biol. Chem.* 278:29633–29639.
19. Zanardelli, S., A. C. Chion, …, D. A. Lane. 2009. A novel binding site for ADAMTS13 constitutively exposed on the surface of globular VWF. *Blood.* 114:2819–2828.
20. Svoboda, K., P. P. Mitra, and S. M. Block. 1994. Fluctuation analysis of motor protein movement and single enzyme kinetics. *Proc. Natl. Acad. Sci. USA*. 91:11782–11786.
21. Gao, W., P. J. Anderson, …, J. E. Sadler. 2006. Exosite interactions contribute to tension-induced cleavage of von Willebrand factor by the antithrombotic ADAMTS13 metalloprotease. *Proc. Natl. Acad. Sci. USA*. 103:19099–19104.
22. Long, M., H. L. Goldsmith, …, C. Zhu. 1999. Probabilistic modeling of shear-induced formation and breakage of doublets cross-linked by receptor-ligand bonds. *Biophys. J.* 76:1112–1128.
23. Gao, W., P. J. Anderson, and J. E. Sadler. 2008. Extensive contacts between ADAMTS13 exosites and von Willebrand factor domain A2 contribute to substrate specificity. *Blood.* 112:1713–1719.